Biochar-Based Adsorption Processes: Considerations for Antibiotics Removal

Subjects: Others

Contributor: Umut Sen , Bruno Esteves , Terencio Aguiar , Helena Pereira

Antibiotics are pharmaceuticals that are used to treat bacterial infections in humans and animals, and they are also used as growth promoters in livestock production. These activities lead to an alarming accumulation of antibiotics in aquatic environments, resulting in selection pressure for antibiotic resistance. Carbon-based materials (mainly in the form of activated carbons, carbon nanotubes, graphene, and biochars) are commonly used for the adsorption of antibiotics because of their four characteristics that contribute to adsorption, including specific surface area, micro- and mesopore structures, surface functional groups;mineral content and composition.

antibiotics biochar tetracycline surface area ash content

1. Biochar Properties

The most relevant properties of biochars in relation to their adsorption ability are the specific surface area (i), the pore size distribution (ii), and surface functional groups (iii) such as hydroxyl, carboxyl, carbonyl, etc. [1]. The mineral content and composition (iv) of biochars are also important in the adsorption of bulky antibiotics such as tetracyclines through surface complexation [2][3].

The biochar's properties contribute to the available active sites for adsorption, improving the adsorption capacity [4]. The pore structure is formed due to the release of volatile compounds and water loss in the dehydration process during pyrolysis. Thus, the feedstock and the pyrolysis conditions, especially the temperature, significantly affect the biochar's pore structure and, consequently, the adsorption capacity of the biochar [5][6][7].

A high pyrolysis temperature has been linked to a larger surface area, higher microporosity, and graphitic structures, due to the increase in volatilization at higher temperatures [8][9][10][11][12]. On the other hand, at low pyrolysis temperatures, the functional groups are retained and they contribute to adsorption [3][13]. Therefore, generally, moderate temperatures (400–700 °C) are more suitable for the development of favorable pore structures [9]. The aromatic carbon groups (C=C), carbonyl groups (C=O), and aliphatic groups (CH_2 + CH_3) were determined for four biochars produced by carbonizing corn crop residue (*Zea mays* L.) and wood shavings of oak (*Quercus* ssp.) at 350 °C and 600 °C using slow pyrolysis. The results showed that the aromatic carbon content increased with temperature for both biochars, while the carbonyl and aliphatic groups decreased [14][15], which is in agreement with the results of Fu et al. [16]. Thus, a high pyrolysis temperature is almost always advantageous for the adsorption process, although the biochar yield decreases with increasing pyrolysis temperature and the economic viability of the process is reduced.

Several pore measurements have been reported for biochars. The most common measure is the total pore volume, which includes all pores. According to the International Union of Pure and Applied Chemistry (IUPAC), pores can be divided into three main groups: micropores (<2 nm), mesopores (2–50 nm), and macropores (>50 nm) [6]. However, some authors also use the term “nanopores” to indicate micropores, probably because they are in the nanometer range. The role of each type of pore in adsorption is different. Macropores are primarily linked to the diffusion of substances, mesopores serve as channels for mass transfer, and micropores provide space for trapping [6][17]. The high temperatures in pyrolysis have been stated to be responsible for the presence of pores with sizes around 1.2 and 1.0 nm—the so-called micropores—leading to an increased surface area [18]. Nevertheless, the surface area only increases with the pyrolysis temperature up to a maximum, after which the surface area decreases [1]. For instance, some authors state that there are two competing phenomena: the first increases the volatile release and, consequently, the surface area; and the other is thermal deactivation that leads to char melting, pore fusion, and structure ordering, which decrease the surface area and pore volume [19][20][21].

The heating rate is also important in the formation of the pore structure. For example, tests conducted at two different heating rates (10–30 °C/min and 50 °C/min) showed that at the lower heating rate the volatiles formed were released from the surface, leading to an open fiber structure with the formation of cavities and, therefore, increasing the surface area [22]. On the other hand, a higher heating rate led to a decrease in surface area and pore volume, which was believed to be due to some of the pore walls becoming too thin and breaking [22]. The same effect was also observed with pyrolysis residence time. Thus, the severity of the pyrolysis conditions (i.e., maximum pyrolysis temperature, heating rate, and solid residence time) increases the surface area to some extent, but it decreases after a certain limit (which is dependent on biomass, chemical and anatomical composition, and the heat and mass transfer rate). This phenomenon has two practical implications: (i) it is not always necessary to apply the most severe conditions, and (ii) energy savings can be achieved by applying the optimal pyrolysis conditions.

The determination of the surface area available for adsorption faces some problems. For instance, the prevailing method to determine the surface area, N_2 adsorption at 77 K, has a kinetic diffusion limitation for N_2 in small micropores [23]. The kinetic limitation arises from the inflexibility of the matrix, leading to an artificially lower surface area for some chars. This phenomenon has been reported by several authors, for instance for oak, pine, and grass chars, where the N_2 surface area was 225, 285, and 77 m^2/g, respectively, while the CO_2 area for the same materials was 528, 843, and 427 m^2/g, respectively [24]. Similar results were presented for sewage sludge and wood chip char [25]. The higher surface area estimation by CO_2 has been reported to be due to the higher kinetic energy associated with the smaller kinetic diameter of CO_2 (3.3 Å vs. 3.64 Å for CO_2 and N_2, respectively), which allows CO_2 to diffuse more easily into the small pores [24][26][27].

Argon has also been used to measure char’s surface area at 77 K and 87 K. The results showed that at 87 K the surface area was slightly greater than at 77 K, which was attributed to the increased mobility of Ar molecules at higher temperatures. On the other hand, the low values of surface area measured by Ar were believed to be due to the lower amount of mesopores [28].

The size of the pores also affects the sorption, because the filling of micropores involves a higher number of contact points than the filling of mesopores, and pore filling has been characterized as being influenced by size exclusion effects [23]. A comparison of the adsorption-relevant properties of different biochars is presented in **Table 1**.

Table 1. Pyrolysis temperature, char yield, surface properties, and ash content of different biochars.

Feedstock	Pyrolysis Temperature (°C)	Char Yield (%)	Surface Area m^2/g	Pore Volume cm^3/g	Ash Content (%)	Reference
Sewage sludge	750	-	60.7		-	[29]
Sewage sludge	400	76.1	23.7		-	[30]
Sewage sludge	600	-	92.3		-	[31]
Sewage sludge	500	-	25.4	0.056	74.2	[32]
	900		67.6	0.099	88.1	
Sewage sludge	700	65	26.70	0.159	86.8	[33]
Palm oil mill sludge	400	54.2	47.7	0.007	44.8	[34]
	800	-	193.1	0.065	59.5	
Pine needles	400	30	112.4	0.044	2.3	[18]
	700	14	490.8	0.186	2.2	
Pine needles	700	25	390	0.12	18.7	[8]
Used tea leaves	350–550	-	8.1	0.012	-	[35]
Ponderosa pine wood	500	28.4	196		2.1	[36]
Ponderosa pine wood	700	22.0	347		1.7	
Tall fescue straw	700	28.8	139		19.3	
Quercus lobata wood	650		225		3.7	[24]
			285			
Pinus taeda wood			77 (N_2)		1.1	

Feedstock	Pyrolysis Temperature (°C)	Char Yield (%)	Surface Area m^2/g	Pore Volume cm^3/g	Ash Content (%)	Reference
Tripsacum floridanum grass			528		15.9	
			643			
			427 (CO_2)			
Beech wood	800	12.5 ± 0.2	70.2	0.003	-	[21]
	1200	10.0 ± 0.7	110.2	0.047		
	1600	8.3 ± 0.4	48.7	0.040		
	2000	8.3 ± 0.5	22.2	0.032		
Poplar wood	600	-	411	0.182	4.7	[22]
Durian wood (*Durio zibethinus*)	550	24.6	221	0.008	20.8	[37]
Paulownia elongata wood	-	-	310		4.1	[38]
Pinewood sawdust (*Pinus radiata*)	800	11.6	738.0	0.244	1.9	[39]
Oak bark	450	22.8	1.9	1.060	11.3	[40]
Corn stover	450	15	12		58.0	[41]
Corn stover	500	17	3.1		32.4	[42]
Soybean stover	700	21.6	420.3	0.190	17.2	[43]
Cotton stalk	500		1.5	0.007	2.7	[16]
Duckweed	500	44	12	0.014	9.5	[44]
Rice husk	500	-	34.4	0.028	42.2	[45]
Rice husk	550	-	181		-	[46]
Rice straw	400	-	4.4	0.015	40.7	[47]

Feedstock	Pyrolysis Temperature (°C)	Char Yield (%)	Surface Area m^2/g	Pore Volume cm^3/g	Ash Content (%)	Reference
	700		161.2	0.086	52.5	
Rice straw	700	-	20.6	0.019	-	[48]
Rapeseed	550	-	25.4 (BET) 18.3 (Micro) 7.1 (Meso)	0.0480	24.9	[49]
Rapeseed	700	29.6	19.3	1.254	14.4	[50]
Maize	600	29.54	70	0.06	27.2	[51]
Sugarcane bagasse (SGB)	300	-	224.1		4.2	[52]
	400		361.8		4.2	
	500		291.4		4.1	
Giant *Miscanthus*	500	27.2	181		-	[53]
	700	25.1	369			
Peanut shell	700	21.9	448.2	0.200	8.9	[43]
Palm kernel shell	400	46.7	4.5	0.011	8.1	[12]
	500	37.5	12	0.086	5.2	
	600	35.4	260	0.17	8.9	
	700	32.8	370	0.19	8.4	
Olive stones	400	-	476.3		36.2	[54]
	600		173.3		41.2	
Alfalfa (*Medicago sativa*)	500	-	31.1		31.3	[55]
Orange peel	700	22.2	201.0	0.035	2.8	[56]
Tire rubber	400	59.3	24.2	0.080	15.4	[57]
	600	54.5	51.5	0.120	15.6	

Feedstock	Pyrolysis Temperature (°C)	Char Yield (%)	Surface Area m^2/g	Pore Volume cm^3/g	Ash Content (%)	Reference
	800	43.0	50.0	0.110	10.5	
Grape seeds	700	28	124 (N_2)		-	[28]
			454 (CO_2)			
			66 (Ar77)			
	600	31	110 (N_2)			
			424 (CO_2)			
			57 (Ar77)			
Wood	600	23.3	127		1.3	[58]
Straw		25.2	22		24.5	
Green waste		24.4	46		13.4	
Dry algae		22.9	19		73.0	
Cow manure	500	57.2	21.9	0.028	67.5	[59]
Pig manure		38.5	47.4	0.075	48.4	
Shrimp hull		33.4	13.3	0.039	53.8	
Bone dregs		48.7	113	0.278	77.6	
Wastewater sludge		45.9	71.6	0.060	61.9	
Waste paper		36.6	133	0.084	53.5	
Sawdust		28.3	203	0.125	9.9	
Grass		27.8	3.33	0.010	20.8	
Wheat straw		29.8	33.2	0.051	18.0	
Peanut shell		32.0	43.5	0.040	10.6	
Chlorella		40.2	2.78	0.010	52.6	
Waterweeds		58.4	3.78	0.009	63.5	
Spruce wood	525	-	40.4		4.7	[60]

Feedstock	Pyrolysis Temperature (°C)	Char Yield (%)	Surface Area m^2/g	Pore Volume cm^3/g	Ash Content (%)	Reference
Poplar wood			55.7		6.8	
Wheat straw			14.2		12.7	
Pine sawdust (air lim.)	300		12.1		6.7	
Maize straw (air lim.)	300		7.8		15.4	
SCB (air lim.)	300		25.3		11.8	
Pine sawdust N_2	300	-	8.2		4.6	[61]
Maize straw N_2	300		2.6		11.3	
SCB N_2	300		12.2		8.9	
Pine sawdust N_2	500		68.4		6.9	
Maize straw N_2	500		33.2		17.6	
SCB N_2	500		97.8		12.3	
Wheat straw		24.6	177	0.110	12.0	
Corn straw	600	26.7	7	0.012	18.0	[62]
Peanut-shell		28.5	185	0.110	11.0	
Broiler litter	350	-	60.0	0.000	-	[63]
	700		94	0.018		
Poultry litter	600	46	5.79		60.8	[64]
Feedlot manure	700	32.2	145.2		92.0	[11]
Goat-manure	600	37.9	13.9	0.008	-	[65]
	800	33.8	93.5	0.049		
Yak manure	700	-	82.9	0.074	-	[66]
S. dimorphus	500	-	123		43.3	[67]
Microalgae	600		89		44.2	

Feedstock	Pyrolysis Temperature (°C)	Char Yield (%)	Surface Area m^2/g	Pore Volume cm^3/g	Ash Content (%)	Reference
Laminaria japonica microalgae	600	38.0	79.9	0.044	55.1	[68]
Waste marine	400	67.7	70.3	0.112	41.9	
Macroalgae	600	47.8	61.8	0.078	48.7	[69]
(*Undaria pinnatifida* roots)	800	39.3	44.5	0.057	50.4	
Saccharina japonica macroalgae	600	-	266 (unwashed) 543 (washed)	0.132 0.266	-	[70]
Bamboo Industrial waste	550 650 750 850 950	-	277.3 266.7 228.6 382.8 143.4 (S_{BET}) 221.6 228.7 200.8 320.7 99.7 (S_{mic})	0.173 0.162 0.144 0.254 0.142	-	[71]
Rice straw	700	30.7	32.9 [74]	0.049	-	[72]
Pig manure		38	20.5	0.045		
Douglas fir wood	600	16.0	500	0.2	-	[73]
Hybrid poplar wood		20.4	416	0.17		

d applied

hars, and

s used in har is the mprove its s, pH, etc. erestingly, activation

[75][76][77]

processes [1].

Currently, different physical or chemical modifications (**Table 2**) are applied to biochars to improve their adsorption capacity [78]. These modifications are discussed below.

thods.

Feedstock	Pyrolysis Temperature (°C)	Char Yield (%)	Surface Area m^2/g	Pore Volume cm^3/g	Ash Content (%)	Reference

Treatment No.	Treatment	Advantages	Disadvantages
1	Acid treatment	Removal of metals; increased surface area	Lower biochar yield due to acid hydrolysis; inefficient removal of silica; high cost
2	Alkali treatment	Removal of silica; increased surface area	Lower biochar yield due to alkaline hydrolysis; inefficient removal of metals; high cost
3	Demineralization with hot water	Efficient removal of metals and silica	Energy- and time-consuming; additional drying step required
4	Ball milling	Increased surface area	High cost; less effective than chemical methods
5	Steam activation	Increased surface area	Reduced biochar yield
6	Doping with organic compounds	Addition of surface functional groups	High cost
7	Surfactant modification	Addition of acidic or basic surface functional groups	Leaching of surfactant; high cost
8	Mineral impregnation	Addition of metal oxides on the biochar surface	Secondary contamination by leaching of mineral
9	Mineral impregnation: iron	Addition of iron atoms on the biochar surface; easy removal of magnetic particles from water	Secondary contamination by leaching of iron
10	Composite-forming clays	Enhanced ion-exchange mechanism	Environmental impact of clay processing
11	Composite-forming by carbon	Addition of adsorption sites	High cost
12	Composite-forming by heteroatom doping	Addition of surface functional groups	High cost; heteroatom leaching; specialized process

Treatment No.	Treatment	Advantages	Disadvantages
13	Molecular imprinting	Production of a specialized type of biochar selective to target (imprint) molecules; reusable	High cost; specialized process

l porosity. d surface icro- and mesopores inside the biochar's structure (ii), and removing the inorganic compounds (iii) [5][79][80][81].

Acid–base combined treatments can be considered for low-porosity biochars bearing limited surface functional groups, such as municipal sewage sludge biochars [5][82][83]. These treatments seem to be superior to the single acid or alkali treatments [5]. However, the available data are still scarce. More experimental results with a broader range of biochars are required to better understand the effects of the combined acid–base treatments.

Physical treatment methods, such as coating with carbonaceous materials, ball milling, and template formation, can also result in surface enhancement. Ball milling seems to be a feasible method to produce biochar nanoparticles [84]. Future research should focus on developing technologies to simultaneously achieve enhanced functionality and porous structure of biochars.

Cationic or anionic surfactants such as cetyltrimethylammonium bromide (CTAB) and sodium dodecyl sulfate (SDS) are used to alter the adsorbent's surface and, in particular, to change the surface charge [85]. Certain organic compounds, such as humic acid (HA) [86], methanol [87], and chitosan [88][89][90], have been used in the modification of biochars because they introduce supplementary functional groups (e.g., carbonyl (-C=O-), amino ($-NH_2$) and hydroxyl (-OH)) to the surface of biochar [5]. However, organic compound modification has cost disadvantages, which limit its development [5]. Metal or metal oxide modification provides a higher number of adsorption sites and creates a larger surface area in biochars [5][82][91][92][93]. The metal modification is particularly effective in the recycling of biochars after adsorption. However, metal modifications generate contamination of water bodies through metal ion shedding [5].

Doping with carbonaceous materials is the introduction of carbonaceous materials (e.g., graphene and carbon nanotubes) into the surface structure of biochars to improve their adsorption efficiency [5][94]. The increased number of adsorption sites and the increased specific surface area of the biochar improve its adsorption capacity [5][95][96]. However, graphene, graphene oxide, and carbon nanotubes are highly expensive materials and cannot be considered practical for large-scale adsorption applications [5].

Non-metallic or heteroatom doping of biochars using nitrogen [97][98][99], oxygen [98], sulfur [99], or phosphorus [98] is an efficient modification method to offer increase the stability and adsorption efficiency of adsorbents [5]. The heteroatom doping of biochar provides additional surface functional groups and active sites for adsorption. However, the available research is currently scarce [5].

Other physical modifications, such as steam activation [100] and ball milling [94][101], generate a higher specific surface area, a higher number of functional groups, and pores in biochars. Physical modifications are

environmentally friendly, as they do not use any chemicals during biochar modification [5]. However, they are comparatively less effective than chemical modifications [5].

Molecular imprinting improves the specific adsorption of biochars by creating selective active sites [5]. Molecularly imprinted biochars can be used to remove low-concentration and highly toxic pollutants [5][102]. Molecularly imprinted biochars have already been used to detect and quantify antibiotic residues at trace levels in food and environmental samples [5][103][104]. Molecularly imprinted biochars are reusable, which is their major advantage compared to other biochars [105]. Similar to other modified biochars, molecularly imprinted biochars usually exhibit better adsorption properties for antibiotics than pristine biochars [5].

3. Biochar-Based Antibiotic Adsorption Studies

In the bibliometric survey section, it was shown that antibiotic adsorption studies are increasing in number, while in the antibiotics and bacterial cytology section, antibiotics were grouped into different classes based on their chemical structure. It is important to observe the adsorption studies of each major antibiotic group. **Figure 1** provides an overview of adsorption studies with different antibiotics. Adsorption studies were predominantly performed on tetracycline, fluoroquinolone, and sulfonamide antibiotics. This is consistent with the co-occurrence map and suggests that these antibiotics are selective to carbonaceous adsorbents.

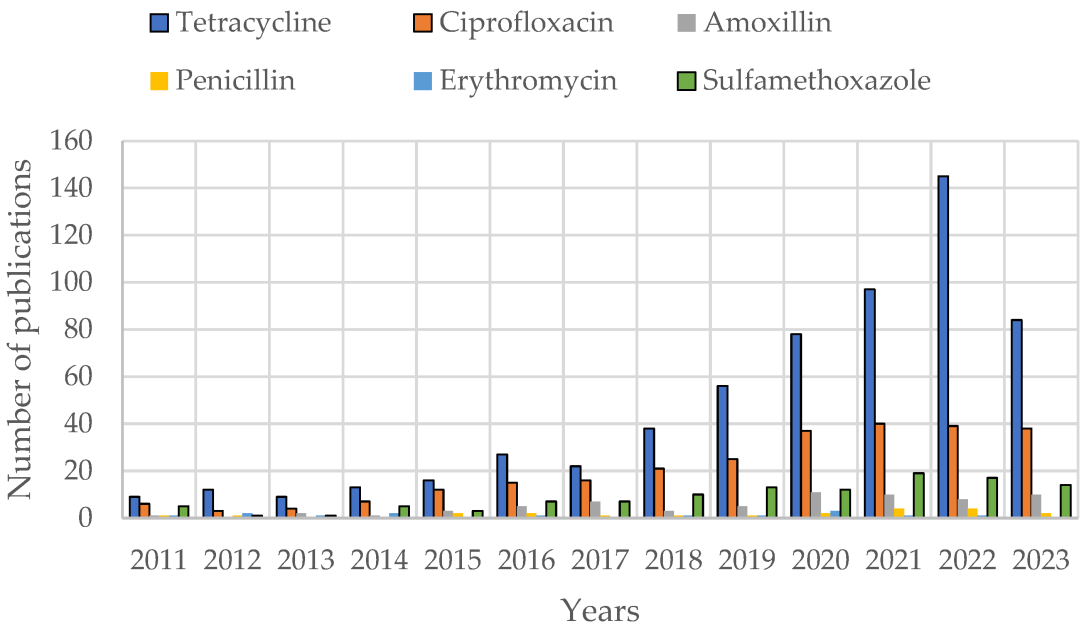

Figure 1. Number of publications with “adsorption” and “different antibiotics” titles on the Web of Science (WOS).

Previous studies on biochar-based removal of antibiotics were mainly performed on modified biochars. The usage of pristine biochars for the removal of antibiotics is currently limited to biochars prepared by pyrolysis, which are termed pristine biochars (PBs) [1]. However, in order to modify the adsorption performance of biochars, the first

step is to understand the adsorption performance of pristine biochars by studying the biochars' properties and adsorption mechanisms.

The adsorption mechanisms of different carbonaceous materials are not identical, although certain mechanisms, such as π–π electron donor–acceptor (EDA) interactions and hydrogen bonding, are considered both for high-surface-area carbon nanotubes and for biochars, indicating the role of intermolecular interactions in the adsorption [106]. According to Du et al. (2023), at least seven different mechanisms, including hydrogen bonding, π–π interactions, surface complexation, electrostatic interactions, pore filling, ion exchange, and hydrophobic interactions, can contribute to the adsorption of antibiotics onto biochars [5]. This excellent review also showed that antibiotic adsorption studies with biochars were mostly performed with modified biochars (approximately 65% of the studies) [5].

Table 3 provides a comparison of proposed antibiotic adsorption mechanisms and maximum adsorption capacities for pristine biochars and modified biochars.

Table 3. Mechanisms of antibiotic adsorption onto biochars; modified from [78].

Biochar Biochar Precursor	Pyrolysis Temperature (°C)	Proposed Mechanism	Modification	Antibiotic Used	Maximum Adsorption Capacity (Q_m) (mg/g)	Reference
Pristine biochars						
Pinus radiata wood sawdust	600–800	n.a	n.a	Tetracycline (TC)	163	[39]
Bamboo sawdust	500	n.a	n.a	Enrofloxacin (EF)	45.9 (EF)	[107]
				Ofloxacin (OF)	45.1 (OF)	
Spent coffee grounds	200–700	π–π EDA	n.a	Sulfadiazine (SDZ), sulfamethoxazole (SMX)	0.12 (SDZ) 0.13 (SMX)	[108]
Modified biochars						
Sunflower seed husk	600	Multiple: chemisorption,	H_3PO_4	Tetracycline (TC), ciprofloxacin (CIP),	429.3	[109]

Biochar Biochar Precursor	Pyrolysis Temperature (°C)	Proposed Mechanism	Modification	Antibiotic Used	Maximum Adsorption Capacity (Q_m) (mg/g)	Reference
		external diffusion, intraparticle diffusion		sulfamethoxazole (SMX)	(TC) 361.6 (CIP) 251.3 (SMX)	
Bamboo	380	Hydrogen bonds, π–π EDA, Lewis acid–base	H_3PO_4	Sulfamethoxazole (SMX)	88.10	[110]
Poplar wood	500	Pore filling, π–π interactions, surface complexation, hydrogen bonding, and electrostatic interactions	KOH Fe_3O_4	Tetracyclines (TCs)	70.3–89.6 (TCs)	[111]
				Fluoroquinolones (FQs)	35.5–60.3 (FQs)	
Palm fibers	500	Pore filling, surface electrostatic interactions, hydrogen bonding complexation, and π–π EDA interactions	Fe–N co-doped	Sulfamethoxazole (SMX)	42.9	[112]

dsorption
teractions

4. Thermodynamic and Kinetic Considerations

Thermodynamic and kinetic (rate and mechanism) studies are the two essential tools in adsorption studies because they answer fundamental questions such as whether an adsorption process works, how it works, how to optimize it, and how to design better adsorbents.

Thermodynamics determines the feasibility of an adsorption process under various temperature and pressure conditions. The thermodynamic analysis of adsorption involves the calculation of thermodynamic parameters such as Gibbs free energy, enthalpy, and entropy (ΔG, ΔH, and ΔS, respectively), which can be used to assess the thermodynamic feasibility of the adsorption process. For instance,

- If ΔG < 0, the process is thermodynamically favorable, and adsorption will occur spontaneously;
- If ΔG > 0, the process is thermodynamically unfavorable, and adsorption will not occur spontaneously:

- If $\Delta G = 0$, the process is at thermodynamic equilibrium.

Enthalpy change (ΔH) is another thermodynamic parameter that is used to assess the feasibility of adsorption. If the adsorption is exothermic ($\Delta H < 0$), it releases heat and is more favorable at lower temperatures. If the adsorption is endothermic ($\Delta H > 0$), it absorbs heat and is more favorable at higher temperatures. Entropy change (ΔS) is the final factor to assess the feasibility of adsorption. An increase in entropy ($\Delta S > 0$) favors the adsorption process.

These factors are related according to the following equation:

$$\Delta G = \Delta H - T\Delta S$$

In order for ΔG to be negative, either the enthalpy change (ΔH) should be negative (exothermic process) and greater than the $T\Delta S$ product (typically positive), or, in the case of endothermic reactions, the entropy change (ΔS) should be large enough to offset the positive enthalpy change (ΔH) and temperatures (T) should be high.

Exothermic adsorption ($\Delta H < 0$) involves relatively strong adsorbate–surface interactions, such as chemical sorption or strong van der Waals forces, while endothermic adsorption involves weak adsorbate–surface interactions such as physical sorption (weak intermolecular interactions). The entropy change (ΔS) may be positive or negative in chemical sorption, but it is usually negative in physical sorption.

Pressure can also affect the adsorption process, but its impact in liquid adsorption is less pronounced than temperature. High pressures increase the entropy and favor the adsorption process, but they may also lead to degradation of the adsorbent.

Thus, in order to optimize the adsorption of antibiotics onto biochars, it is necessary to calculate the thermodynamic properties. If the adsorption is exothermic, it should be performed at low temperatures, and if the adsorption is endothermic it should be performed at high temperatures. If the adsorption occurs due to surface chemical reactions, the adsorbent's surface should be modified with metal oxides or heteroatoms to increase the number of available complexation sites and drive the adsorption process in a thermodynamically favorable manner. If the adsorption occurs through physical sorption, oxygenated surface functional groups should be introduced to the biochars to increase the intermolecular interactions, such as hydrogen bonds. It should be noted that the adsorption of antibiotics is a complex reaction and involves both surface chemical reactions and physical sorption [109]. Therefore, different experimental conditions should be tested to optimize the adsorption process.

A particular case of thermodynamic studies is the study of adsorption isotherms that describe the equilibrium relationship between the concentration of adsorbate molecules and the amount of adsorbate adsorbed onto the surface of the adsorbent. Thus, they provide information about the adsorption capacity and the adsorbent–adsorbate surface interactions. The Langmuir isotherm and Freundlich isotherm are the most frequently used adsorption isotherms. According to the Langmuir isotherm, the adsorbent's surface is homogeneous, and adsorption occurs as a monolayer until all available sites are occupied by adsorbate molecules and there are no

interactions among the adsorbed molecules. The Freundlich isotherm assumes a heterogeneous adsorbent surface, multilayer adsorption, and interactions among the adsorbed molecules.

Kinetic models of adsorption describe how adsorbate molecules are adsorbed onto the surface of an adsorbent material as a function of time. The kinetic models explain the reaction rate and the mechanisms, and they provide insights into the dynamic aspects of adsorption. The most frequently used kinetic models are the pseudo-first-order model, pseudo-second-order model, Elovich model, and intraparticle diffusion model. The pseudo-first-order and pseudo-second-order models consider the surface reaction as the rate-liming step, while the intraparticle diffusion model considers the intraparticle diffusion as the rate limiting step. According to the pseudo-first-order kinetic model, the adsorption rate (dq/dt) is proportional to the difference between the equilibrium concentration (qe) and the concentration at a given time (q), while according to the pseudo-second-order kinetic model the adsorption rate is proportional to the square difference between the equilibrium concentration and the concentration at a given time. The Elovich model assumes that rate of the adsorption is not constant over time and that there are interactions between the adsorbate molecules. The intraparticle diffusion model describes the rate of intraparticle diffusion.

The adsorption of tetracycline antibiotics onto zinc chloride activated biochar was described by the pseudo-second-order kinetic model and the Langmuir isotherm, with a maximum (monolayer) adsorption capacity of 200 mg/g tetracycline. Hydrogen bonding and electrostatic interactions were the main proposed mechanisms [113]. The adsorption of quinolone antibiotics onto magnetic biochar also resulted in a similar trend. The adsorption was described by the pseudo-second-order kinetic model and the Langmuir isotherm, with a maximum adsorption capacity of 68.9 mg/g [114]. Similarly, the adsorption of tetracycline, quinolone, and sulfonamide antibiotics onto H_3PO_4 activated biochar was described well by the Elovich and pseudo-second-order kinetic models, as well as by the Langmuir isotherm [109]. Interestingly the results of this latter study indicated that the adsorption of antibiotics is an endothermic and spontaneous process with negative Gibbs free energy and a positive entropy change. Both chemical and physical adsorption occurred simultaneously [109]. The endothermic character of antibiotic adsorption on activated carbon was also reported for the adsorption of heavy metals [115]. On the other hand, the adsorption of sulfonamide antibiotics onto H_3PO_4 activated biochar resulted in a spontaneous and exothermic process that was favorable at low temperatures [116]. The adsorption was described by the Langmuir isotherm and the pseudo-second-order kinetic model, similar to previous studies [116]. The study of Srivastava et al. (2002) also showed a similar trend. The adsorption of quinolone and tetracycline antibiotics onto modified biochar was exothermic and was described by the Langmuir isotherm and the pseudo-second-order kinetic model [117].

The above examples were the modified biochars, which are the biochars most frequently used as adsorbents. The kinetic models and isotherms for the adsorption of antibiotics onto pristine biochars seem to follow the same trend (i.e., Langmuir isotherm and pseudo-second-order kinetics). However, there are still few studies on pristine biochars providing insights into their adsorption mechanisms. For instance, the adsorption of tetracycline antibiotics onto wheat-stalk biochars was described well with the Langmuir isotherm as well as the pseudo-second-order and intraparticle diffusion kinetic models [84]. A similar kinetic model was reported for the adsorption of sulfonamide antibiotics onto a biochar based on spent coffee grounds. The adsorption kinetics of sulfadiazine (SDZ) and

sulfamethoxazole (SMX), two common sulfonamide antibiotics, was better described by a pseudo-second-order model, implying that the adsorption of antibiotics onto biochars is controlled by the chemisorption mechanism [108].

The overall results indicate that the adsorption of antibiotics onto pristine or modified biochars predominantly occurs as a monolayer through surface reactions and intraparticle diffusion mechanisms. Thermodynamic studies of the adsorption of different antibiotics have shown that the adsorption of antibiotics on biochars can be exothermic or endothermic and should be determined for each adsorption case to improve the adsorption efficiency.

References

1. Wang, B.; Gao, B.; Fang, J. Recent advances in engineered biochar productions and applications. Crit. Rev. Environ. Sci. Technol. 2017, 47, 2158–2207.
2. Ji, L.; Wan, Y.; Zheng, S.; Zhu, D. Adsorption of tetracycline and sulfamethoxazole on crop residue-derived ashes: Implication for the relative importance of black carbon to soil sorption. Environ. Sci. Technol. 2011, 45, 5580–5586.
3. Qiu, B.; Shao, Q.; Shi, J.; Yang, C.; Chu, H. Application of biochar for the adsorption of organic pollutants from wastewater: Modification strategies, mechanisms and challenges. Sep. Purif. Technol. 2022, 300, 121925.
4. Weber, K.; Quicker, P. Properties of biochar. Fuel 2018, 217, 240–261.
5. Du, L.; Ahmad, S.; Liu, L.; Wang, L.; Tang, J. A review of antibiotics and antibiotic resistance genes (ARGs) adsorption by biochar and modified biochar in water. Sci. Total Environ. 2023, 858, 159815.
6. Leng, L.; Xiong, Q.; Yang, L.; Li, H.; Zhou, Y.; Zhang, W.; Jiang, S.; Li, H.; Huang, H. An overview on engineering the surface area and porosity of biochar. Sci. Total Environ. 2021, 763, 144204.
7. Bagreev, A.; Bandosz, T.J.; Locke, D.C. Pore structure and surface chemistry of adsorbents obtained by pyrolysis of sewage sludge-derived fertilizer. Carbon N. Y. 2001, 39, 1971–1979.
8. Ahmad, M.; Rajapaksha, A.U.; Lim, J.E.; Zhang, M.; Bolan, N.; Mohan, D.; Vithanage, M.; Lee, S.S.; Ok, Y.S. Biochar as a sorbent for contaminant management in soil and water: A review. Chemosphere 2014, 99, 19–33.
9. Braida, W.J.; Pignatello, J.J.; Lu, Y.; Ravikovitch, P.I.; Neimark, A.V.; Xing, B. Sorption hysteresis of benzene in charcoal particles. Environ. Sci. Technol. 2003, 37, 409–417.
10. Pattaraprakorn, W.; Nakamura, R.; Aida, T.; Niiyama, H. Adsorption of CO2 and N2 onto charcoal treated at different temperatures. J. Chem. Eng. Jpn. 2005, 38, 366–372.

11. Cantrell, K.B.; Hunt, P.G.; Uchimiya, M.; Novak, J.M.; Ro, K.S. Impact of pyrolysis temperature and manure source on physicochemical characteristics of biochar. Bioresour. Technol. 2012, 107, 419–428.
12. Wang, P.; Zhang, J.; Shao, Q.; Wang, G. Physicochemical properties evolution of chars from palm kernel shell pyrolysis. J. Therm. Anal. Calorim. 2018, 133, 1271–1280.
13. Ahmad, S.; Gao, F.; Lyu, H.; Ma, J.; Zhao, B.; Xu, S.; Ri, C.; Tang, J. Temperature-dependent carbothermally reduced iron and nitrogen doped biochar composites for removal of hexavalent chromium and nitrobenzene. Chem. Eng. J. 2022, 450, 138006.
14. Nguyen, B.T.; Lehmann, J. Black carbon decomposition under varying water regimes. Org. Geochem. 2009, 40, 846–853.
15. Nguyen, B.T.; Lehmann, J.; Hockaday, W.C.; Joseph, S.; Masiello, C.A. Temperature sensitivity of black carbon decomposition and oxidation. Environ. Sci. Technol. 2010, 44, 3324–3331.
16. Fu, P.; Hu, S.; Xiang, J.; Sun, L.; Su, S.; An, S. Study on the gas evolution and char structural change during pyrolysis of cotton stalk. J. Anal. Appl. Pyrolysis 2012, 97, 130–136.
17. Chen, Y.; Zhang, X.; Chen, W.; Yang, H.; Chen, H. The structure evolution of biochar from biomass pyrolysis and its correlation with gas pollutant adsorption performance. Bioresour. Technol. 2017, 246, 101–109.
18. Chen, B.; Zhou, D.; Zhu, L. Transitional adsorption and partition of nonpolar and polar aromatic contaminants by biochars of pine needles with different pyrolytic temperatures. Environ. Sci. Technol. 2008, 42, 5137–5143.
19. Kim, K.H.; Kim, J.-Y.; Cho, T.-S.; Choi, J.W. Influence of pyrolysis temperature on physicochemical properties of biochar obtained from the fast pyrolysis of pitch pine (Pinus rigida). Bioresour. Technol. 2012, 118, 158–162.
20. Lu, L.; Kong, C.; Sahajwalla, V.; Harris, D. Char structural ordering during pyrolysis and combustion and its influence on char reactivity. Fuel 2002, 81, 1215–1225.
21. Zeng, K.; Minh, D.P.; Gauthier, D.; Weiss-Hortala, E.; Nzihou, A.; Flamant, G. The effect of temperature and heating rate on char properties obtained from solar pyrolysis of beech wood. Bioresour. Technol. 2015, 182, 114–119.
22. Chen, D.; Li, Y.; Cen, K.; Luo, M.; Li, H.; Lu, B. Pyrolysis polygeneration of poplar wood: Effect of heating rate and pyrolysis temperature. Bioresour. Technol. 2016, 218, 780–788.
23. Lattao, C.; Cao, X.; Mao, J.; Schmidt-Rohr, K.; Pignatello, J.J. Influence of molecular structure and adsorbent properties on sorption of organic compounds to a temperature series of wood chars. Environ. Sci. Technol. 2014, 48, 4790–4798.

24. Mukherjee, A.; Zimmerman, A.R.; Harris, W. Surface chemistry variations among a series of laboratory-produced biochars. Geoderma 2011, 163, 247–255.
25. Krahn, K.M.; Cornelissen, G.; Castro, G.; Arp, H.P.H.; Asimakopoulos, A.G.; Wolf, R.; Holmstad, R.; Zimmerman, A.R.; Sørmo, E. Sewage sludge biochars as effective PFAS-sorbents. J. Hazard. Mater. 2023, 445, 130449.
26. Mehio, N.; Dai, S.; Jiang, D. Quantum mechanical basis for kinetic diameters of small gaseous molecules. J. Phys. Chem. A 2014, 118, 1150–1154.
27. Pignatello, J.J.; Kwon, S.; Lu, Y. Effect of natural organic substances on the surface and adsorptive properties of environmental black carbon (char): Attenuation of surface activity by humic and fulvic acids. Environ. Sci. Technol. 2006, 40, 7757–7763.
28. Jimenez-Cordero, D.; Heras, F.; Alonso-Morales, N.; Gilarranz, M.A.; Rodriguez, J.J. Porous structure and morphology of granular chars from flash and conventional pyrolysis of grape seeds. Biomass Bioenergy 2013, 54, 123–132.
29. Jindarom, C.; Meeyoo, V.; Kitiyanan, B.; Rirksomboon, T.; Rangsunvigit, P. Surface characterization and dye adsorptive capacities of char obtained from pyrolysis/gasification of sewage sludge. Chem. Eng. J. 2007, 133, 239–246.
30. Zhang, W.; Mao, S.; Chen, H.; Huang, L.; Qiu, R. Pb (II) and Cr (VI) sorption by biochars pyrolyzed from the municipal wastewater sludge under different heating conditions. Bioresour. Technol. 2013, 147, 545–552.
31. Xu, Q.; Tang, S.; Wang, J.; Ko, J.H. Pyrolysis kinetics of sewage sludge and its biochar characteristics. Process Saf. Environ. Prot. 2018, 115, 49–56.
32. Chen, T.; Zhang, Y.; Wang, H.; Lu, W.; Zhou, Z.; Zhang, Y.; Ren, L. Influence of pyrolysis temperature on characteristics and heavy metal adsorptive performance of biochar derived from municipal sewage sludge. Bioresour. Technol. 2014, 164, 47–54.
33. Yuan, H.; Lu, T.; Huang, H.; Zhao, D.; Kobayashi, N.; Chen, Y. Influence of pyrolysis temperature on physical and chemical properties of biochar made from sewage sludge. J. Anal. Appl. Pyrolysis 2015, 112, 284–289.
34. Iberahim, N.; Sethupathi, S.; Bashir, M.J.K. Optimization of palm oil mill sludge biochar preparation for sulfur dioxide removal. Environ. Sci. Pollut. Res. 2018, 25, 25702–25714.
35. Li, J.; Yu, G.; Pan, L.; Li, C.; You, F.; Xie, S.; Wang, Y.; Ma, J.; Shang, X. Study of ciprofloxacin removal by biochar obtained from used tea leaves. J. Environ. Sci. 2018, 73, 20–30.
36. Keiluweit, M.; Nico, P.S.; Johnson, M.G.; Kleber, M. Dynamic molecular structure of plant biomass-derived black carbon (biochar). Environ. Sci. Technol. 2010, 44, 1247–1253.

37. Chowdhury, Z.Z.; Karim, M.Z.; Ashraf, M.A.; Khalid, K. Influence of carbonization temperature on physicochemical properties of biochar derived from slow pyrolysis of durian wood (Durio zibethinus) sawdust. BioResources 2016, 11, 3356–3372.
38. Vaughn, S.F.; Kenar, J.A.; Tisserat, B.; Jackson, M.A.; Joshee, N.; Vaidya, B.N.; Peterson, S.C. Chemical and physical properties of Paulownia elongata biochar modified with oxidants for horticultural applications. Ind. Crops Prod. 2017, 97, 260–267.
39. Li, C.; Zhu, X.; He, H.; Fang, Y.; Dong, H.; Lü, J.; Li, J.; Li, Y. Adsorption of two antibiotics on biochar prepared in air-containing atmosphere: Influence of biochar porosity and molecular size of antibiotics. J. Mol. Liq. 2019, 274, 353–361.
40. Mohan, D.; Rajput, S.; Singh, V.K.; Steele, P.H.; Pittman, C.U., Jr. Modeling and evaluation of chromium remediation from water using low cost bio-char, a green adsorbent. J. Hazard. Mater. 2011, 188, 319–333.
41. Lee, J.W.; Kidder, M.; Evans, B.R.; Paik, S.; Buchanan, A.C., III; Garten, C.T.; Brown, R.C. Characterization of biochars produced from cornstovers for soil amendment. Environ. Sci. Technol. 2010, 44, 7970–7974.
42. Mullen, C.A.; Boateng, A.A.; Goldberg, N.M.; Lima, I.M.; Laird, D.A.; Hicks, K.B. Bio-oil and bio-char production from corn cobs and stover by fast pyrolysis. Biomass Bioenergy 2010, 34, 67–74.
43. Ahmad, M.; Lee, S.S.; Dou, X.; Mohan, D.; Sung, J.-K.; Yang, J.E.; Ok, Y.S. Effects of pyrolysis temperature on soybean stover-and peanut shell-derived biochar properties and TCE adsorption in water. Bioresour. Technol. 2012, 118, 536–544.
44. Muradov, N.; Fidalgo, B.; Gujar, A.C.; Garceau, N.; Ali, T. Production and characterization of Lemna minor bio-char and its catalytic application for biogas reforming. Biomass Bioenergy 2012, 42, 123–131.
45. Liu, P.; Liu, W.-J.; Jiang, H.; Chen, J.-J.; Li, W.-W.; Yu, H.-Q. Modification of bio-char derived from fast pyrolysis of biomass and its application in removal of tetracycline from aqueous solution. Bioresour. Technol. 2012, 121, 235–240.
46. Cope, C.O.; Webster, D.S.; Sabatini, D.A. Arsenate adsorption onto iron oxide amended rice husk char. Sci. Total Environ. 2014, 488, 554–561.
47. Deng, Y.; Huang, S.; Dong, C.; Meng, Z.; Wang, X. Competitive adsorption behaviour and mechanisms of cadmium, nickel and ammonium from aqueous solution by fresh and ageing rice straw biochars. Bioresour. Technol. 2020, 303, 122853.
48. Zeng, Z.; Tan, X.; Liu, Y.; Tian, S.; Zeng, G.; Jiang, L.; Liu, S.; Li, J.; Liu, N.; Yin, Z. Comprehensive adsorption studies of doxycycline and ciprofloxacin antibiotics by biochars prepared at different temperatures. Front. Chem. 2018, 6, 80.

49. Angın, D.; Şensöz, S. Effect of pyrolysis temperature on chemical and surface properties of biochar of rapeseed (Brassica napus L.). Int. J. Phytoremedia. 2014, 16, 684–693.
50. Karaosmanoğlu, F.; Işığıgür-Ergüdenler, A.; Sever, A. Biochar from the straw-stalk of rapeseed plant. Energy Fuels 2000, 14, 336–339.
51. Wang, X.; Zhou, W.; Liang, G.; Song, D.; Zhang, X. Characteristics of maize biochar with different pyrolysis temperatures and its effects on organic carbon, nitrogen and enzymatic activities after addition to fluvo-aquic soil. Sci. Total Environ. 2015, 538, 137–144.
52. Mubarik, S.; Saeed, A.; Athar, M.M.; Iqbal, M. Characterization and mechanism of the adsorptive removal of 2, 4, 6-trichlorophenol by biochar prepared from sugarcane baggase. J. Ind. Eng. Chem. 2016, 33, 115–121.
53. Lee, Y.; Ryu, C.; Park, Y.-K.; Jung, J.-H.; Hyun, S. Characteristics of biochar produced from slow pyrolysis of Geodae-Uksae 1. Bioresour. Technol. 2013, 130, 345–350.
54. Saldarriaga, J.F.; Montoya, N.A.; Estiati, I.; Aguayo, A.T.; Aguado, R.; Olazar, M. Unburned material from biomass combustion as low-cost adsorbent for amoxicillin removal from wastewater. J. Clean. Prod. 2021, 284, 124732.
55. Jang, H.M.; Kan, E. A novel hay-derived biochar for removal of tetracyclines in water. Bioresour. Technol. 2019, 274, 162–172.
56. Chen, B.; Chen, Z. Sorption of naphthalene and 1-naphthol by biochars of orange peels with different pyrolytic temperatures. Chemosphere 2009, 76, 127–133.
57. Lian, F.; Huang, F.; Chen, W.; Xing, B.; Zhu, L. Sorption of apolar and polar organic contaminants by waste tire rubber and its chars in single-and bi-solute systems. Environ. Pollut. 2011, 159, 850–857.
58. Ronsse, F.; Van Hecke, S.; Dickinson, D.; Prins, W. Production and characterization of slow pyrolysis biochar: Influence of feedstock type and pyrolysis conditions. GCB Bioenergy 2013, 5, 104–115.
59. Zhao, L.; Cao, X.; Mašek, O.; Zimmerman, A. Heterogeneity of biochar properties as a function of feedstock sources and production temperatures. J. Hazard. Mater. 2013, 256, 1–9.
60. Kloss, S.; Zehetner, F.; Dellantonio, A.; Hamid, R.; Ottner, F.; Liedtke, V.; Schwanninger, M.; Gerzabek, M.H.; Soja, G. Characterization of slow pyrolysis biochars: Effects of feedstocks and pyrolysis temperature on biochar properties. J. Environ. Qual. 2012, 41, 990–1000.
61. Luo, L.; Xu, C.; Chen, Z.; Zhang, S. Properties of biomass-derived biochars: Combined effects of operating conditions and biomass types. Bioresour. Technol. 2015, 192, 83–89.
62. Gai, X.; Wang, H.; Liu, J.; Zhai, L.; Liu, S.; Ren, T.; Liu, H. Effects of feedstock and pyrolysis temperature on biochar adsorption of ammonium and nitrate. PLoS ONE 2014, 9, e113888.

63. Uchimiya, M.; Wartelle, L.H.; Lima, I.M.; Klasson, K.T. Sorption of deisopropylatrazine on broiler litter biochars. J. Agric. Food Chem. 2010, 58, 12350–12356.
64. Song, W.; Guo, M. Quality variations of poultry litter biochar generated at different pyrolysis temperatures. J. Anal. Appl. Pyrolysis 2012, 94, 138–145.
65. Touray, N.; Tsai, W.-T.; Chen, H.-R.; Liu, S.-C. Thermochemical and pore properties of goat-manure-derived biochars prepared from different pyrolysis temperatures. J. Anal. Appl. Pyrolysis 2014, 109, 116–122.
66. Zhang, J.; Huang, B.; Chen, L.; Li, Y.; Li, W.; Luo, Z. Characteristics of biochar produced from yak manure at different pyrolysis temperatures and its effects on the yield and growth of highland barley. Chem. Speciat. Bioavailab. 2018, 30, 57–67.
67. Bordoloi, N.; Narzari, R.; Sut, D.; Saikia, R.; Chutia, R.S.; Kataki, R. Characterization of bio-oil and its sub-fractions from pyrolysis of Scenedesmus dimorphus. Renew. Energy 2016, 98, 245–253.
68. Jung, K.-W.; Jeong, T.-U.; Kang, H.-J.; Ahn, K.-H. Characteristics of biochar derived from marine macroalgae and fabrication of granular biochar by entrapment in calcium-alginate beads for phosphate removal from aqueous solution. Bioresour. Technol. 2016, 211, 108–116.
69. Jung, K.-W.; Kim, K.; Jeong, T.-U.; Ahn, K.-H. Influence of pyrolysis temperature on characteristics and phosphate adsorption capability of biochar derived from waste-marine macroalgae (Undaria pinnatifida roots). Bioresour. Technol. 2016, 200, 1024–1028.
70. Boakye, P.; Tran, H.N.; Lee, D.S.; Woo, S.H. Effect of water washing pretreatment on property and adsorption capacity of macroalgae-derived biochar. J. Environ. Manag. 2019, 233, 165–174.
71. Yang, H.; Huan, B.; Chen, Y.; Gao, Y.; Li, J.; Chen, H. Biomass-based pyrolytic polygeneration system for bamboo industry waste: Evolution of the char structure and the pyrolysis mechanism. Energy Fuels 2016, 30, 6430–6439.
72. Liu, Y.; Yao, S.; Wang, Y.; Lu, H.; Brar, S.K.; Yang, S. Bio-and hydrochars from rice straw and pig manure: Inter-comparison. Bioresour. Technol. 2017, 235, 332–337.
73. Suliman, W.; Harsh, J.B.; Abu-Lail, N.I.; Fortuna, A.-M.; Dallmeyer, I.; Garcia-Perez, M. Influence of feedstock source and pyrolysis temperature on biochar bulk and surface properties. Biomass Bioenergy 2016, 84, 37–48.
74. Ok, Y.S.; Chang, S.X.; Gao, B.; Chung, H.-J. SMART biochar technology—A shifting paradigm towards advanced materials and healthcare research. Environ. Technol. Innov. 2015, 4, 206–209.
75. Mohamed, B.A.; Ellis, N.; Kim, C.S.; Bi, X.; Emam, A.E. Engineered biochar from microwave-assisted catalytic pyrolysis of switchgrass for increasing water-holding capacity and fertility of sandy soil. Sci. Total Environ. 2016, 566, 387–397.

76. Yao, Y.; Gao, B.; Chen, J.; Yang, L. Engineered biochar reclaiming phosphate from aqueous solutions: Mechanisms and potential application as a slow-release fertilizer. Environ. Sci. Technol. 2013, 47, 8700–8708.
77. Rajapaksha, A.U.; Chen, S.S.; Tsang, D.C.W.; Zhang, M.; Vithanage, M.; Mandal, S.; Gao, B.; Bolan, N.S.; Ok, Y.S. Engineered/designer biochar for contaminant removal/immobilization from soil and water: Potential and implication of biochar modification. Chemosphere 2016, 148, 276–291.
78. Xiang, Y.; Xu, Z.; Wei, Y.; Zhou, Y.; Yang, X.; Yang, Y.; Yang, J.; Zhang, J.; Luo, L.; Zhou, Z. Carbon-based materials as adsorbent for antibiotics removal: Mechanisms and influencing factors. J. Environ. Manag. 2019, 237, 128–138.
79. Huang, H.; Tang, J.; Gao, K.; He, R.; Zhao, H.; Werner, D. Characterization of KOH modified biochars from different pyrolysis temperatures and enhanced adsorption of antibiotics. RSC Adv. 2017, 7, 14640–14648.
80. Nguyen, V.-T.; Nguyen, T.-B.; Huang, C.P.; Chen, C.-W.; Bui, X.-T.; Dong, C.-D. Alkaline modified biochar derived from spent coffee ground for removal of tetracycline from aqueous solutions. J. Water Process Eng. 2021, 40, 101908.
81. Zhang, X.; Gang, D.D.; Zhang, J.; Lei, X.; Lian, Q.; Holmes, W.E.; Zappi, M.E.; Yao, H. Insight into the activation mechanisms of biochar by boric acid and its application for the removal of sulfamethoxazole. J. Hazard. Mater. 2022, 424, 127333.
82. Tang, L.; Yu, J.; Pang, Y.; Zeng, G.; Deng, Y.; Wang, J.; Ren, X.; Ye, S.; Peng, B.; Feng, H. Sustainable efficient adsorbent: Alkali-acid modified magnetic biochar derived from sewage sludge for aqueous organic contaminant removal. Chem. Eng. J. 2018, 336, 160–169.
83. Zhou, Y.; He, Y.; He, Y.; Liu, X.; Xu, B.; Yu, J.; Dai, C.; Huang, A.; Pang, Y.; Luo, L. Analyses of tetracycline adsorption on alkali-acid modified magnetic biochar: Site energy distribution consideration. Sci. Total Environ. 2019, 650, 2260–2266.
84. Xiang, W.; Wan, Y.; Zhang, X.; Tan, Z.; Xia, T.; Zheng, Y.; Gao, B. Adsorption of tetracycline hydrochloride onto ball-milled biochar: Governing factors and mechanisms. Chemosphere 2020, 255, 127057.
85. Gęca, M.; Khalil, A.M.; Tang, M.; Bhakta, A.K.; Snoussi, Y.; Nowicki, P.; Wiśniewska, M.; Chehimi, M.M. Surface Treatment of Biochar—Methods, Surface Analysis and Potential Applications: A Comprehensive Review. Surfaces 2023, 6, 179–213.
86. Zhao, J.; Liang, G.; Zhang, X.; Cai, X.; Li, R.; Xie, X.; Wang, Z. Coating magnetic biochar with humic acid for high efficient removal of fluoroquinolone antibiotics in water. Sci. Total Environ. 2019, 688, 1205–1215.

87. Jing, X.-R.; Wang, Y.-Y.; Liu, W.-J.; Wang, Y.-K.; Jiang, H. Enhanced adsorption performance of tetracycline in aqueous solutions by methanol-modified biochar. Chem. Eng. J. 2014, 248, 168–174.
88. Gao, N.; Du, W.; Zhang, M.; Ling, G.; Zhang, P. Chitosan-modified biochar: Preparation, modifications, mechanisms and applications. Int. J. Biol. Macromol. 2022, 209, 31–49.
89. Liu, J.; Zhou, B.; Zhang, H.; Ma, J.; Mu, B.; Zhang, W. A novel Biochar modified by Chitosan-Fe/S for tetracycline adsorption and studies on site energy distribution. Bioresour. Technol. 2019, 294, 122152.
90. Ngo, H.H.; Guo, W.; Nguyen, T.H.; Luong, T.M.L.; Nguyen, X.H.; Phan, T.L.A.; Nguyen, M.P.; Nguyen, M.K. New chitosan-biochar composite derived from agricultural waste for removing sulfamethoxazole antibiotics in water. Bioresour. Technol. 2023, 385, 129384.
91. Hu, B.; Tang, Y.; Wang, X.; Wu, L.; Nong, J.; Yang, X.; Guo, J. Cobalt-gadolinium modified biochar as an adsorbent for antibiotics in single and binary systems. Microchem. J. 2021, 166, 106235.
92. Shen, Q.; Wang, Z.; Yu, Q.; Cheng, Y.; Liu, Z.; Zhang, T.; Zhou, S. Removal of tetracycline from an aqueous solution using manganese dioxide modified biochar derived from Chinese herbal medicine residues. Environ. Res. 2020, 183, 109195.
93. Xiang, Y.; Yang, X.; Xu, Z.; Hu, W.; Zhou, Y.; Wan, Z.; Yang, Y.; Wei, Y.; Yang, J.; Tsang, D.C.W. Fabrication of sustainable manganese ferrite modified biochar from vinasse for enhanced adsorption of fluoroquinolone antibiotics: Effects and mechanisms. Sci. Total Environ. 2020, 709, 136079.
94. Amusat, S.O.; Kebede, T.G.; Dube, S.; Nindi, M.M. Ball-milling synthesis of biochar and biochar–based nanocomposites and prospects for removal of emerging contaminants: A review. J. Water Process Eng. 2021, 41, 101993.
95. Huang, D.; Wang, X.; Zhang, C.; Zeng, G.; Peng, Z.; Zhou, J.; Cheng, M.; Wang, R.; Hu, Z.; Qin, X. Sorptive removal of ionizable antibiotic sulfamethazine from aqueous solution by graphene oxide-coated biochar nanocomposites: Influencing factors and mechanism. Chemosphere 2017, 186, 414–421.
96. Inyang, M.; Gao, B.; Zimmerman, A.; Zhou, Y.; Cao, X. Sorption and cosorption of lead and sulfapyridine on carbon nanotube-modified biochars. Environ. Sci. Pollut. Res. 2015, 22, 1868–1876.
97. Mei, Y.; Xu, J.; Zhang, Y.; Li, B.; Fan, S.; Xu, H. Effect of Fe–N modification on the properties of biochars and their adsorption behavior on tetracycline removal from aqueous solution. Bioresour. Technol. 2021, 325, 124732.
98. Tang, W.; Zanli, B.L.G.L.; Chen, J. O/N/P-doped biochar induced to enhance adsorption of sulfonamide with coexisting Cu2+/Cr (VI) by air pre-oxidation. Bioresour. Technol. 2021, 341,

125794.

99. Zhang, Y.; Liang, S.; He, R.; Zhao, J.; Lv, J.; Kang, W.; Zhang, J. Enhanced adsorption and degradation of antibiotics by doping corncob biochar/PMS with heteroatoms at different preparation temperatures: Mechanism, pathway, and relative contribution of reactive oxygen species. J. Water Process Eng. 2022, 46, 102626.
100. Wang, R.-Z.; Huang, D.-L.; Liu, Y.-G.; Zhang, C.; Lai, C.; Wang, X.; Zeng, G.-M.; Zhang, Q.; Gong, X.-M.; Xu, P. Synergistic removal of copper and tetracycline from aqueous solution by steam-activated bamboo-derived biochar. J. Hazard. Mater. 2020, 384, 121470.
101. Huang, J.; Zimmerman, A.R.; Chen, H.; Gao, B. Ball milled biochar effectively removes sulfamethoxazole and sulfapyridine antibiotics from water and wastewater. Environ. Pollut. 2020, 258, 113809.
102. Wu, B.; Wan, J.; Zhang, Y.; Pan, B.; Lo, I.M.C. Selective phosphate removal from water and wastewater using sorption: Process fundamentals and removal mechanisms. Environ. Sci. Technol. 2019, 54, 50–66.
103. Tarannum, N.; Khatoon, S.; Dzantiev, B.B. Perspective and application of molecular imprinting approach for antibiotic detection in food and environmental samples: A critical review. Food Control 2020, 118, 107381.
104. Wang, Q.; Wang, T.; Zhang, Y.; Ma, J.; Tuo, Y. Preparation and evaluation of a chitosan modified biochar as an efficient adsorbent for pipette tip-solid phase extraction of triazine herbicides from rice. Food Chem. 2022, 396, 133716.
105. Lehmann, J.; Joseph, S. Biochar for Environmental Management: Science, Technology and Implementation; Routledge: Abingdon, UK, 2015; ISBN 1134489536.
106. Liao, P.; Zhan, Z.; Dai, J.; Wu, X.; Zhang, W.; Wang, K.; Yuan, S. Adsorption of tetracycline and chloramphenicol in aqueous solutions by bamboo charcoal: A batch and fixed-bed column study. Chem. Eng. J. 2013, 228, 496–505.
107. Wang, Y.; Lu, J.; Wu, J.; Liu, Q.; Zhang, H.; Jin, S. Adsorptive removal of fluoroquinolone antibiotics using bamboo biochar. Sustainability 2015, 7, 12947–12957.
108. Zhang, X.; Zhang, Y.; Ngo, H.H.; Guo, W.; Wen, H.; Zhang, D.; Li, C.; Qi, L. Characterization and sulfonamide antibiotics adsorption capacity of spent coffee grounds based biochar and hydrochar. Sci. Total Environ. 2020, 716, 137015.
109. Nguyen, T.-B.; Chen, W.-H.; Chen, C.-W.; Patel, A.K.; Bui, X.-T.; Chen, L.; Singhania, R.R.; Dong, C.-D. Phosphoric acid-activated biochar derived from sunflower seed husk: Selective antibiotic adsorption behavior and mechanism. Bioresour. Technol. 2023, 371, 128593.

110. Ahmed, M.B.; Zhou, J.L.; Ngo, H.H.; Guo, W.; Johir, M.A.H.; Sornalingam, K. Single and competitive sorption properties and mechanism of functionalized biochar for removing sulfonamide antibiotics from water. Chem. Eng. J. 2017, 311, 348–358.
111. Zhang, X.; Zhen, D.; Liu, F.; Chen, R.; Peng, Q.; Wang, Z. An achieved strategy for magnetic biochar for removal of tetracyclines and fluoroquinolones: Adsorption and mechanism studies. Bioresour. Technol. 2023, 369, 128440.
112. Diao, Y.; Shan, R.; Li, M.; Gu, J.; Yuan, H.; Chen, Y. Efficient Adsorption of a Sulfonamide Antibiotic in Aqueous Solutions with N-doped Magnetic Biochar: Performance, Mechanism, and Reusability. ACS Omega 2022, 8, 879–892.
113. Wang, H.; Lou, X.; Hu, Q.; Sun, T. Adsorption of antibiotics from water by using Chinese herbal medicine residues derived biochar: Preparation and properties studies. J. Mol. Liq. 2021, 325, 114967.
114. Kong, X.; Liu, Y.; Pi, J.; Li, W.; Liao, Q.; Shang, J. Low-cost magnetic herbal biochar: Characterization and application for antibiotic removal. Environ. Sci. Pollut. Res. 2017, 24, 6679–6687.
115. Azari, A.; Kakavandi, B.; Kalantary, R.R.; Ahmadi, E.; Gholami, M.; Torkshavand, Z.; Azizi, M. Rapid and efficient magnetically removal of heavy metals by magnetite-activated carbon composite: A statistical design approach. J. Porous Mater. 2015, 22, 1083–1096.
116. Meng, Q.; Zhang, Y.; Meng, D.; Liu, X.; Zhang, Z.; Gao, P.; Lin, A.; Hou, L. Removal of sulfadiazine from aqueous solution by in-situ activated biochar derived from cotton shell. Environ. Res. 2020, 191, 110104.
117. Srivastava, A.; Dave, H.; Prasad, B.; Maurya, D.M.; Kumari, M.; Sillanpää, M.; Prasad, K.S. Low cost iron modified syzygium cumini l. Wood biochar for adsorptive removal of ciprofloxacin and doxycycline antibiotics from aqueous solution. Inorg. Chem. Commun. 2022, 144, 109895.